

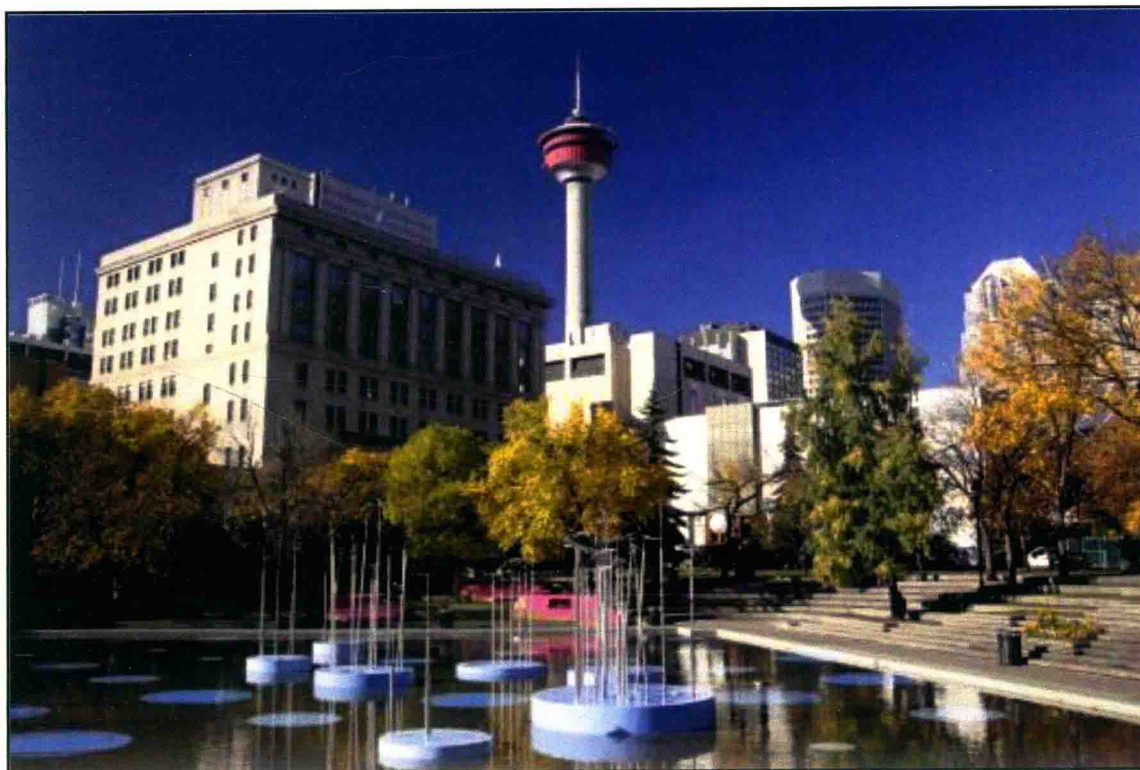
# TSOP 2017

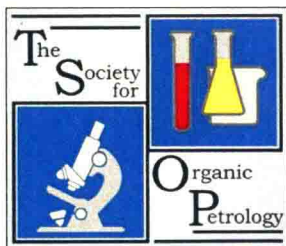
---

**Annual Meeting of The Society for Organic Petrology**  
**September 21-27, 2017**  
**Calgary, Alberta, Canada**

---

Hosted by the Canadian Society for Coal Science and Organic Petrology





## **TSOP 2017**

**September 21-27, 2017**

**Hyatt Regency Hotel, Calgary Alberta Canada**

### **CONTENTS**

Calendar of Events

Floor Plan

Oral program

Poster Program

Abstracts for Oral Presentations

Abstracts for Poster Presentations

### **LOCAL ORGANIZING COMMITTEE**

Chairs: Hamed Sanei, Judith Potter

Treasurer: David L. Marchioni

Budget: Judith Potter

Technical program: Hamed Sanei, Lavern Stasiuk,

Field Trip Coordinators: David Marchioni, Bill McDougall, Jennifer Galloway, Judith Potter

Registration: Julito Reyes

Website: Jillian Verbeught

Software management: Mark Obermajer

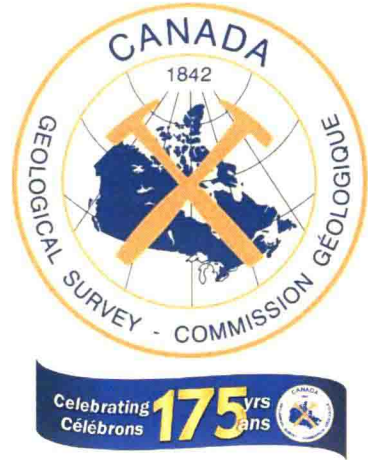
Student Events: Danielle Kondla

Members at large: Dane Synnott, Sarah Saad, Katherine Clark, Anne Nguyen, Kristine Evans,  
Dennis Jiang, Mastaneh Liseroudi

The Local Organizing Committee, TSOP 2017, gratefully acknowledges the generosity of our

## SPONSORS

### Diamond Sponsorship



### Silver Sponsorship



### Bronze Sponsorship

*Jp PetroGraphics*

## List of Exhibitors

**CRAIC Technologies**



**Geological Survey of Canada**



**Renishaw Inc.**



**Wildcat Technologies**



# TSOP 2017

September 21-27, 2017

Hyatt Regency Hotel, Calgary Alberta Canada

## CALENDAR OF EVENTS

Thursday, Sept 21:

8.00 am                      Pre-meeting Field Trip: Coals of the Lower Cretaceous Horseshoe Canyon Formation, Southern Alberta Plains region and the Royal Tyrrell Museum of Palaeontology  
Departing from Wynham Hotel-Calgary Airport.

Friday, Sept 22:

|                |   |   |
|----------------|---|---|
| 8.30 - 5.00 pm | Registration  | Grand Foyer (3 <sup>rd</sup> Floor)         |
| 8.30 - 5.00 pm | Short Course: Applications of Organic Petrography in the North American shale petroleum systems | Imperial 4 (3 <sup>rd</sup> Floor)          |
| 6.00 - 8.30pm  | Icebreaker  | Atrium (3 <sup>rd</sup> Floor)              |
| 7.30 -10.30pm  | Outgoing Council Meeting  | Imperial Ballroom 4 (3 <sup>rd</sup> Floor) |

Saturday, Sept 23:

|                  |                         |   |
|------------------|-------------------------|---|
| 8.30 - 12.30 pm  | Technical Presentations | Imperial Ballroom 6/8 (3 <sup>rd</sup> Floor) |
| 10.30 - 10.50 am | Morning coffee break    | Grand Foyer (3 <sup>rd</sup> Floor)           |
| 1.30 - 5.00pm    | Technical Presentations | Imperial Ballroom 4 (3 <sup>rd</sup> Floor)   |
| 3.00 – 3.20 pm   | Afternoon coffee break  | Grand Foyer (3 <sup>rd</sup> Floor)           |
| 8.30 – 5.00pm    | Poster session          | Grand Foyer (3 <sup>rd</sup> Floor)           |
| 6.30 – 10.30pm   | Conference Dinner       | Thompsons Restaurant, Main Floor              |

**Sunday, Sept 24:**

|                        |                                 |   |
|------------------------|---------------------------------|---|
| <b>8.30 - 12.30 pm</b> | <b>Technical Presentations</b>  | <b>Imperial Ballroom 4 (3<sup>rd</sup> Floor)</b>     |
| 10.30 - 10.50 am       | Morning coffee break            | Grand Foyer (3 <sup>rd</sup> Floor)                   |
| <b>12.00 – 1.30pm</b>  | <b>Business Luncheon</b>        | <b>Imperial ballroom 5/6/7 (3<sup>rd</sup> Floor)</b> |
| <b>1.30 - 5.00pm</b>   | <b>Technical Presentations</b>  | <b>Imperial Ballroom 6/8 (3<sup>rd</sup> Floor)</b>   |
| 3.00 – 3.20 pm         | Afternoon coffee break          | Grand Foyer (3 <sup>rd</sup> Floor)                   |
| <b>8.30 – 5.00pm</b>   | <b>Poster session</b>           | <b>Grand Foyer (3<sup>rd</sup> Floor)</b>             |
| <b>6.30 - 10.30pm</b>  | <b>incoming Council Meeting</b> | <b>Neilson 3 (3<sup>rd</sup> Floor)</b>               |

**Monday, Sept 25:**

|                       |                                |                             |
|-----------------------|--------------------------------|-----------------------------|
| <b>8:30 departure</b> | <b>Post-meeting Field Trip</b> | <b>Lobby of Hyatt Hotel</b> |
|-----------------------|--------------------------------|-----------------------------|

THURSDAY-September 21, 2017

Pre-Meeting Field Trip: Meet in lobby of Wyndham Hotel-Calgary Airport 7:30 -7:45 am (with luggage)-Bus departs at 8:00am

FRIDAY-September 22, 2017

Registration: Grand Foyer (3rd Floor), Hyatt, 8:00am - 6:00pm

Short Course: Imperial Ballroom 4 (3rd Floor), Hyatt, 8:00am -

Icebreaker: Atrium (3rd Floor), Hyatt, 6:00 - 8:30pm

Outgoing Council Meeting: Imperial Ballroom 4 (3rd Floor), Hyatt, 7:30 - 10:30pm

SATURDAY-September 23, 2017 (main session)  
Imperial Ballroom 6/8 (3rd Floor), Hyatt

SATURDAY-September 23, 2017 (concurrent session)  
Imperial Ballroom 4 (3rd Floor), Hyatt

|   |          |          |   |   |
|---|----------|----------|---|---|
| Session Chairs: Jennifer Galloway & Danielle Kondla | 8:30 AM  | 8:35 AM  | Welcoming by Co-Chairs and TSOP-CSCOP Presidents                  |   |
|   | 8:35 AM  | 9:15 AM  | Keynote<br>Per Kent Pedersen                                      | Stratigraphy of organic rich marine mudstones, event or genetic stratigraphy. <b>P63</b>  |
|   | 9:15 AM  | 9:40 AM  | Dane Synnott  | Influence of refractory organic matter on source rock hydrocarbon potential: A case study from the Second White Specks and Belle Fourche formations, Alberta, Canada. <b>P66</b>  |
|   | 9:40 AM  | 10:05 AM | Shuangqing Wang   | Revelation of organic matter sources and sedimentary environment characteristics by petrographic analysis of Middle Jurassic Dameigou Formation, northern Gaidam Basin, China. <b>P50</b>   |
|   | 10:05 AM | 10:30 AM | Brooke Johnson  | Pore water redox variability and environmental change recorded by the 14 Ga Velken Formation, Northern Territories, Australia. <b>P31</b>   |
|   | 10:30 AM | 10:50 AM | Coffee Break  |   |
|   | 10:50 AM | 11:15 AM | Marcelina Kondas  | Preliminary results of the palynological investigation of the South Flank Arbuckle Anticline section, Oklahoma, USA. <b>P5</b>  |
|   | 11:15 AM | 11:40 AM | Stephan Hlohowskyj  | Does molybdenum enrichment imply depositional euxinia? New insights from the Montney formation using molybdenum x-ray absorption fine structure. <b>P24</b>   |
|   | 11:40 AM | 12:05 PM | JianYe Yang   | Application of geochemical effects of lanthanide elements in distinguishing rock types and their diagenetic environments. <b>P55</b>  |
|   | 12:05 PM | 1:30 PM  | Lunch Break   |   |
| Session Chairs: Omid H Ardakani & Bethany Kurz      | 1:30 PM  | 2:10 PM  | Keynote<br>Lavern Stasiuk   | Integration of Reflected Light Microscopy and Scanning Electron Microscopy to investigate the development of organic matter hosted pores in natural and laboratory pyrolyzed samples, Eagle Ford Formation, West Texas, U.S.A. <b>P43</b> |
|   | 2:10 PM  | 2:35 PM  | Yong Ma   | Organic matter pore system in the high gas-yielded Longmaxi shales: Do Graptolite-derived organic matter pores play a significant role? <b>P80</b>  |
|   | 2:35 PM  | 3:00 PM  | Brett Valentine   | Reflectance changes due to broad beam ion milling of coals and organic-rich shales: thermal alteration or surface polishing? <b>P80</b>   |
|   | 3:00 PM  | 3:20 PM  | Coffee Break  |   |
|   | 3:20 PM  | 3:45 PM  | Zihui Lei   | Organic-matter pertinent and clay-mineral associated pores evolution and influence on reservoir: A case study of low-matured Silurian Longmaxi shale at Lizhi village, Yunnan province, south China. <b>P29</b>                           |
|   | 3:45 PM  | 4:10 PM  | Leslie Ruppert  | Investigation of Porosity and Wettability of the Marcellus Shale: a Small-angle Neutron Scattering Study. <b>P7</b>   |
|   | 4:10 PM  | 4:35 PM  | Katherine Clarke  | The Evolution of Petrophysical Properties During Thermal Maturation: Examples from the Montney and Duvernay Formations, Alberta, Canada. <b>P7</b>  |
|   | 4:35 PM  | 5:00 PM  | Kouqi Liu   | In-situ Nano-mechanical Characterization of Organic Matter in Shale. <b>P33</b>   |
|   | 5:00 PM  | 6:30 PM  | Poster Session and Exhibitors<br>Grand Foyer 3 (3rd Floor), Hyatt |   |
|   | 7:00 PM  |          | Conference Banquet<br>(Thompson Restaurant, Main Floor, Hyatt)    |   |

|                                   |          |          |                |   |
|-----------------------------------|----------|----------|----------------|---|
| Session Chair: Shifeng Dai        | 10:50 AM | 11:15 AM | Zhenhua Jing   | Effect of liquid oxidants on coal structure and permeability. <b>P29</b>  |
|                                   | 11:15 AM | 11:40 AM | Jienan Pan     | Pore structure, macromolecular structure and adsorption characteristics of tectonically deformed coal. <b>P34</b>                                   |
|                                   | 11:40 AM | 12:05 PM | Li Yunbo       | The measurement and quantitative analysis method of full scale pore structures in coal. <b>P54</b>  |
|                                   | 12:05 PM | 1:30 PM  | Lunch Break    |   |
| Session Chairs: Jian Chen & Wu Li | 2:10 PM  | 2:35 PM  | Zheng Sijian   | Nuclear magnetic resonance T2 cut-off value of coals: a novel method by fractal analysis theory. <b>P61</b>   |
|                                   | 2:35 PM  | 3:00 PM  | Dangyu Song    | Development and distribution of pores and fissures in coal matrix by SEM images analysis. <b>P44</b>  |
|                                   | 3:00 PM  | 3:20 PM  | Coffee Break   |   |
|                                   | 3:20 PM  | 3:45 PM  | Kaydy Pinetown | A study of biogenic methane production from coals in the Sydney Basin, Australia. <b>P41</b>  |
|                                   | 3:45 PM  | 4:10 PM  | Meng Li        | Coalbed methane potential and its geological controls of the Jurassic coals in the Fukang mining area, Southern Junggar Basin, NW China. <b>P34</b> |
|                                   | 4:10 PM  | 4:35 PM  | Fei Ren        | Optimization of shockwave generation in water conditions for coal fracturing. <b>P22</b>  |
|                                   | 4:35 PM  | 5:00 PM  | Zhenyi Ye      | Occurrence Characteristics and Geological Controlling Factors of Coalbed Methane in the North Linyou of Yonglong Mining Area, China. <b>P57</b>     |
|                                   |          |          |                |   |

Synthetic! ✓  
Pred predominate shale to in.

✓ Lavern Stasiuk \*


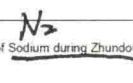
**SUNDAY-September 24, 2017 (main session)**  
Imperial Ballroom 6/8 (Third Floor), Hyatt

|   |          |          |  |  |
|---|----------|----------|--|--|
|   | 8:30 AM  | 8:35 AM  | <b>Meeting Announcements</b>                               |  |
|   | 8:35 AM  | 8:50 AM  | <b>Tribute</b><br>F. Goodarzi,<br>J. Potter,<br>T. Gentzis | Late Professor Duncan Murchison Tribute  |
| Session Chairs: Fari Goodarzi & Shuangqing Wang | 8:50 AM  | 9:15 AM  | Changyi Zhao   | Experimental Study on Hydrocarbon Generation Mechanism of Coal   |
|   | 9:15 AM  | 9:40 AM  | Wu Li  | Hydrocarbon generation from pyrolysis of coals in different rank   |
|   | 9:40 AM  | 10:05 AM | Thomas Gentzis   | A multi-component approach to study the source-rock potential of the Bakken Shale in North Dakota, USA, using organic petrology, Rock-Eval pyrolysis, palynofacies, LmPy-GCMSMS geochemistry, and NMR spectroscopy |
|   | 10:05 AM | 10:30 AM | Louis Tsai   | Depositional and thermal study of a HC containing structure in NW Taiwan   |
|   | 10:30 AM | 10:50 AM | <b>Coffee Break</b>  |  |
|   | 10:50 AM | 11:15 AM | Thomas Gentzis   | Comparative Study of Methylidiamondoid abundances as maturity estimates with conventional maturity proxies: Examples from West Texas and Northern South America  |
|   | 11:15 AM | 11:40 AM | Kouqi Liu  | Understanding Kerogen Mechanical Properties Using Raman Spectroscopy   |
|   | 11:40 AM | 12:05 PM | Yanbin Yao   | A new application of NMR in characterization of multi-phase methane gases and adsorption capacity of shale   |

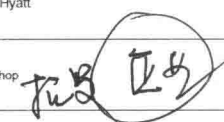
**TSOP 2017 Annual Meeting - Business Luncheon**  
Imperial ballroom 5/7/9 (3rd Floor), Hyatt

|  |          |         |   |  |
|--|----------|---------|---|--|
|  | 12:05 PM | 1:30 PM |   |  |
| Session Chairs: Zhong Ningning & Per K. Pedersen | 1:30 PM  | 2:10 PM | <b>Keynote</b><br>Jim Wood                                    | Hydrocarbon Fluid Distribution in the Montney Tight-Gas Fairway: Modification by Secondary Migration of Methane                  |
|  | 2:10 PM  | 2:35 PM | Kaydy Pinetown  | Gas-water relative wettability of Australian shale   |
|  | 2:35 PM  | 3:00 PM | Kunio Akihisa   | Integrating Mud Gas and Cuttings Analyses to Understand Local CGR Variation in the Montney Tight Gas Reservoir                   |
|  | 3:00 PM  | 3:20 PM | <b>Coffee Break</b>   |  |
|  | 3:20 PM  | 3:45 PM | Deyu Gong   | Geochemical characteristics of natural gases from Southern Junggar Basin, NW China   |
|  | 3:45 PM  | 4:10 PM | Mastaneh Liseroudi  | Late sulfate cements in the Lower Triassic Montney tight gas play and its relation to the origin of sulfate and H <sub>2</sub> S |
|  | 4:10 PM  | 4:35 PM | Kosei Yamaguchi   | Early diagenesis of phosphorus and iron in the meromictic Lake Kai-ike sediments, southwest Japan                                |
|  | 4:35 PM  | 5:00 PM | Dennis Jiang  | Rock-Eval analysis of shale and tight reservoir rock samples: pitfalls and new applications                                      |
|  | 5:00 PM  | 5:30 PM | <b>Closing ceremony</b>                                       |  |
|  | 6:30PM   | 10:30PM | <b>Incoming Council Meeting:</b> Neilson 3 (3rd floor), Hyatt |  |

**SUNDAY-September 24, 2017 (concurrent session)**  
Imperial Ballroom 4 (Third Floor), Hyatt

|  |          |          |                     |  |
|--|----------|----------|---------------------|--|
|  |          |          |                     |  |
| Session Chairs: Anthony Clappaz & Xibo Wang  | 9:15 AM  | 9:40 AM  | Jian Chen           | Mineralogy and geochemistry of the Late Permian No. 5 coals from the Nantong coalfield, Chongqing, southwestern China                                |
|  | 9:40 AM  | 10:05 AM | Fenian Anggara      | Geochemical and REY composition of the coal in Bangko coal field, South Sumatra Basin, Indonesia   |
|  | 10:05 AM | 10:30 AM | Xibo Wang           | Sulfur and Organic Carbon Isotope Compositions of the Early Permian Upper No. 3 Coal from LiangBaosi mine, Southwestern Shandong, China              |
|  | 10:30 AM | 10:50 AM | <b>Coffee Break</b> |  |
|  | 10:50 AM | 11:15 AM | Meili Du            | Study on the Correlation between Trace Elements in Coal and Coal-forming Plants in Yan'an Formation of Middle Jurassic, Ordos Basin                  |
|  | 11:15 AM | 11:40 AM | Yongchun Zhao       | Occurrence and Release of Sodium during Zhundong Coal Combustion  |
|  | 11:40 AM | 12:05 PM | Barbara Bielowicz   | The petrographic analysis of waste generated during the gasification process   |

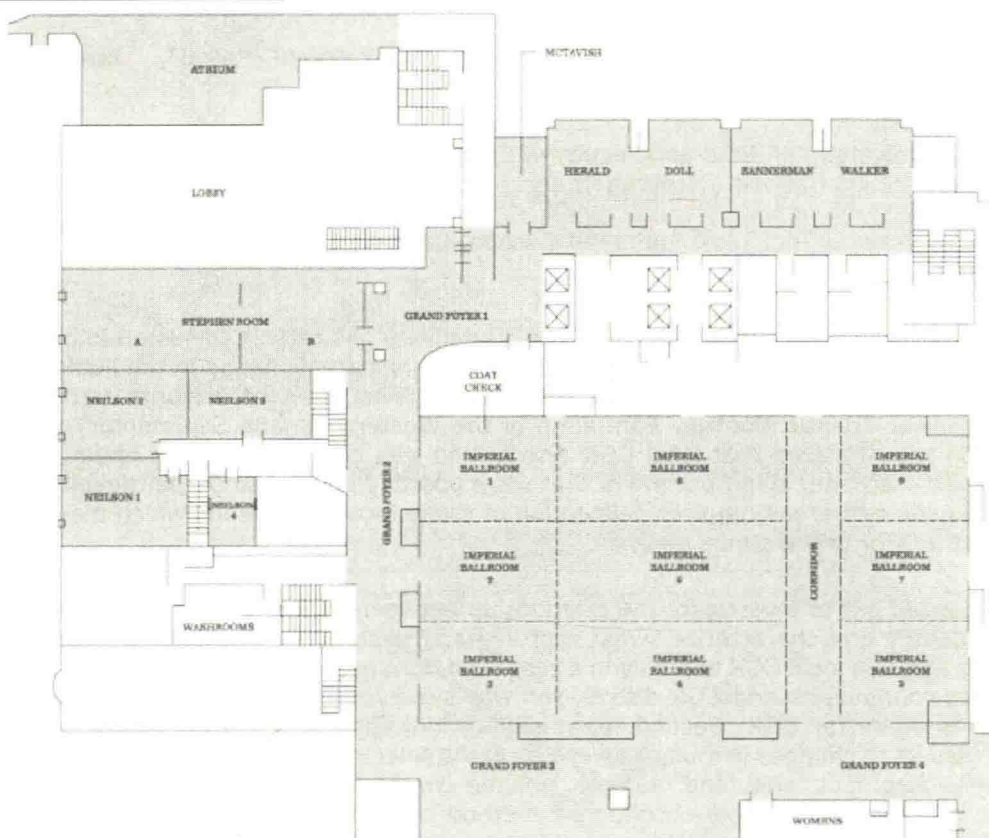
Walker Room, 3rd Floor, Hyatt

|                |         |         |                     |   |
|----------------|---------|---------|---------------------|---|
| RAMAN Workshop | 2:10 PM | 2:35 PM | RAMAN Workshop      | RAMAN Workshop  |
|                | 2:35 PM | 3:00 PM | RAMAN Workshop      | RAMAN Workshop  |
|                | 3:00 PM | 3:20 PM | <b>Coffee Break</b> |   |
|                | 3:20 PM | 3:45 PM | RAMAN Workshop      | RAMAN Workshop  |
|                | 3:45 PM | 4:10 PM | RAMAN Workshop      | RAMAN Workshop  |
|                | 4:10 PM | 4:35 PM | RAMAN Workshop      | RAMAN Workshop  |
|                | 4:35 PM | 5:00 PM | RAMAN Workshop      | RAMAN Workshop  |

**MONDAY-September 25**  
**Post-Meeting Field Trip;** Bus departs Lobby Hyatt Hotel, 8:00am

**MONDAY-September 25-27th**  
**Post-Meeting Field Trip** (Burgess Shale, Mt Stephen), Bus departs Lobby Hyatt Hotel, 8:00am

**Third Floor Room plan**



|                                |  |
|--------------------------------|--|
| <b>Registration desk:</b>      | Grand Foyer 1                                |
| <b>Icebreaker:</b>             | Atrium                                       |
| <b>Technical Sessions:</b>     | Imperial Ballroom 6/8<br>Imperial Ballroom 4 |
| <b>Poster displays:</b>        | Grand Foyer 3-4                              |
| <b>Exhibitors:</b>             | Grand Foyer 3-4                              |
| <b>Raman Demonstration:</b>    | Walker Room                                  |
| <b>TSOP Business Luncheon:</b> | Imperial Ballroom 5/7/9                      |
| <b>Council Meetings:</b>       | Neilson 3                                    |
| <b>Conference Banquet:</b>     | Thompsons Restaurant, main floor             |

# ABSTRACTS FOR ORAL PRESENTATIONS

(Alphabetical order by 1<sup>st</sup> author)

## Integrating Mud Gas and Cuttings Analyses to Understand Local CGR Variation in the Montney Tight Gas Reservoir

Akihisa, Kunio<sup>1\*</sup>, Levi Knapp<sup>2</sup>, Kotaro Sekine<sup>3</sup>, Takashi Akai<sup>3</sup>, James Wood<sup>4</sup>, Omid Haeri Ardakani<sup>5</sup> and Hamed Sanei<sup>5</sup>

<sup>1</sup> Faculty of Mining, University of Akita and Faculty of Engineering, Tokyo University, Japan

<sup>2</sup> Japan Oil, Gas and Metals National Corporation

<sup>4</sup> Encana Corporation

<sup>5</sup> Natural Resources Canada/Geological Survey of Canada, Calgary, Canada

\*presenting author

The liquid content of produced hydrocarbon gas (or condensate gas ratio, CGR) is an important factor for detecting sweet spot areas in tight gas reservoirs. Anomalous areal change in the liquid component of produced hydrocarbon gas, not concordant with the regional thermal maturity trend, has been observed in the Lower Triassic Montney Formation of the Western Canada Sedimentary Basin. Wood and Sanei (2016) hypothesized that local CGR distribution was controlled by the updip migration of thermally degraded methane, along pathways that were possibly influenced by permeability variation. Exploration for liquids-rich areas requires delineation of these local CGR trends which may be possible by using mud gas and/or drill cuttings analysis.

This study was carried out to investigate the relationship between rock properties and gas wetness, in order to better identify and characterize sweet spot areas. The study was conducted in two horizontal wells penetrating across a local CGR anomaly in a silty sand tight gas reservoir (Fig.1). First, the relation between mud gas components and CGR distribution was surveyed to confirm the applicability of mud gas wetness as a proxy for CGR. Second, permeability indices of drill cuttings were analyzed and examined with respect to changes in mud gas wetness in the selected wells (Fig.2). For cuttings analysis, available sample fragment size and sample volume were not necessarily sufficient for NMR measurements, which is regarded as an effective method to analyze permeability. Therefore, careful trial tests were carried out to find suitable sample and measurement conditions. In addition, another permeability index based on solid bitumen saturation and a modified Winland equation was applied to the cuttings analysis (Fig.3). For Montney-type reservoirs, permeability was found to be highly controlled by solid bitumen saturation (Wood et al., 2015). Solid bitumen saturation was calculated using an experimental TOC to solid bitumen relationship. This method converts solid bitumen-derived organic carbon content, measured using Rock-Eval 6, into a solid bitumen saturation value.

In this study area, a strong positive correlation was found between produced gas CGR and mud gas wetness ratio. Mud gas wetness was negatively correlated to cuttings permeability, suggesting methane migration occurred along high permeability, low bitumen saturation pathways. Based on these observations, both mud gas wetness and cuttings permeability indices were confirmed to be effective for detecting liquids-rich areas in immature developing areas.

**Keywords:** CGR wetness-ratio, mud-gas cuttings, permeability, solid-bitumen

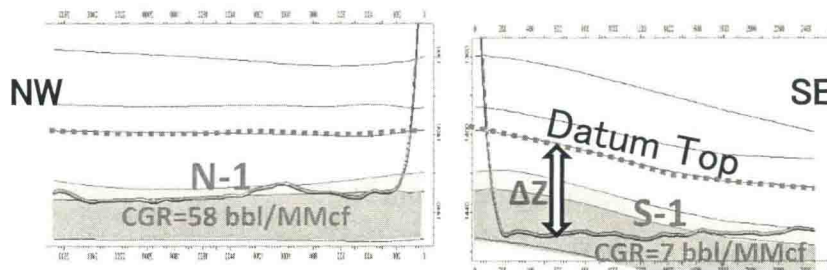


Fig. 1 Horizontal well section crossing a local CGR anomaly area

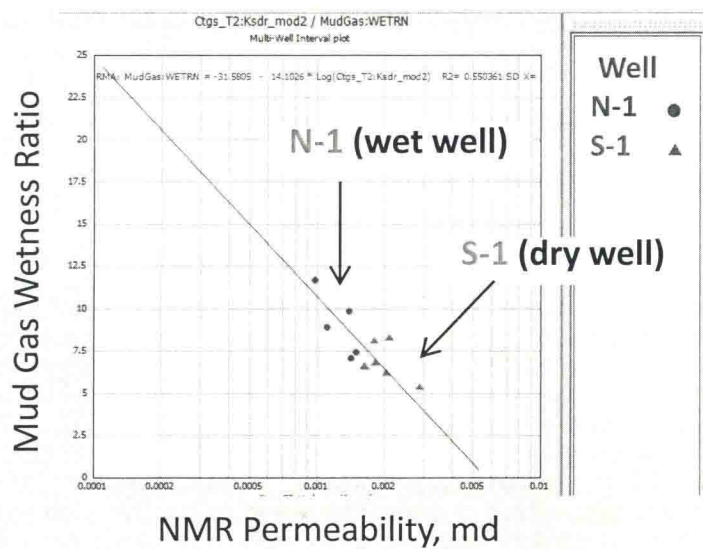


Fig. 2 Cuttings NMR permeability versus mud gas wetness ratio in horizontal wells

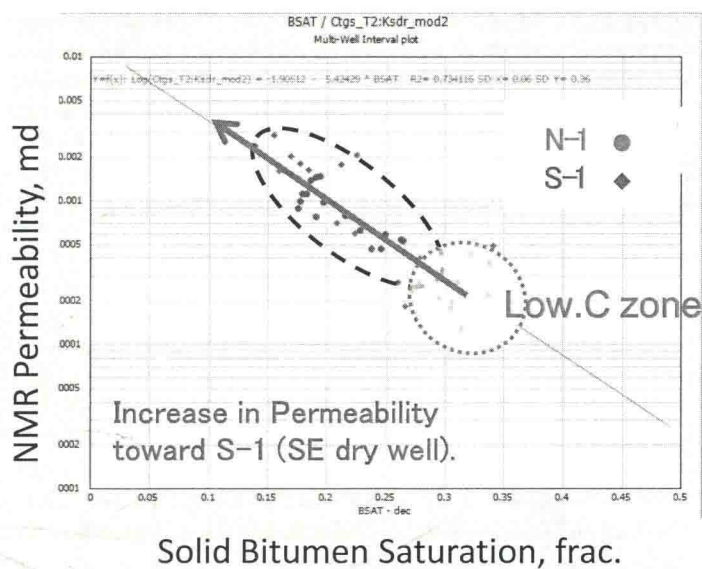


Fig. 3 Solid bitumen saturation versus cuttings NMR permeability

# Geochemical and REY composition of the coal in Bangko coal field, South Sumatra Basin, Indonesia

Anggara, Ferian\*<sup>1</sup>, D. Hendra Amijaya<sup>1</sup>, T. Noely Tambaria and Amanda Sahri

<sup>1</sup> Universitas Gadjah Mada, Yogyakarta, Indonesia

\*presenting author

This paper reports characterisation and process of Rare earth elements and yttrium (REY) enrichment in Banko Coalfield, Tanjung Enim, and South Sumatra, Indonesia. Banko coalfield was a part of South Sumatra basin, which is gets influence of volcanic activity during its peat formation. Volcanic eruptions in the surrounding area produced ash which accumulated as claystone layers or tonsteins in the coal seams. In the Muara Enim Formation, only five main coal seams layer e.g. the A1 and A2 (Mangus) seams, B1 and B2 (Suban) seams as well as C (Petai) seams are considered economic enough to be mined. Banko Coalfield consist of at least 27 coal layers, 14 parting layers and 4 tonsteins layers. The mineralogy of the coal and tonsteins has been evaluated using thin section and qualitative X-ray diffraction (XRD) techniques. Coals and tonsteins are mainly consisting by quartz, kaolinite, and minor boehmite. Result of ICP-AES analysis showing that all tonstein in interseam layer A1 and a tonstein in the lower C seam could be determined as mafic tonstein ( $\text{TiO}_2 / \text{Al}_2\text{O}_3 > 0,08$ ), while a tonstein in the upper C seam determined as alkaline tonstein ( $\text{TiO}_2 / \text{Al}_2\text{O}_3 = 0,02-0,08$ ).

Concentration of REY in Banko Coalfield shows same trend with Chinese and world hard coal, where Ce, La, Nd, and Y has higher content than other rare earth elements. Normalized concentration of REY in Banko Coalfield by upper continental crust (Taylor and McLennan, 1985), showing trend that being more pronounced in HREE. Compared to Chinese coals and to world hard coals, the coal from Banko Coalfield is enriched in  $\text{SiO}_2$  (26.48%),  $\text{Al}_2\text{O}_3$  (11.24%),  $\text{TiO}_2$  (0.35%),  $\text{MnO}$  (0.019%) and has a higher  $\text{SiO}_2 / \text{Al}_2\text{O}_3$  ratio (2.35) due to the higher proportions of quartz compared to the proportions of boehmite or kaolinite in the coal. Inductively coupled plasma-mass spectroscopy (ICP-MS) analysis show the higher REY concentrations found on the coal layers with a thickness less than 0.85 m, while the highest REY in Bangko coal found in the upper C seam, under the layer of alkali tonstein (118.4 ppm). Maceral analysis in the coal under tonstein layers shows higher fusinite, semifusinite, and inertodetrinite, since it was formed in the well drained swamp areas. The coal contains quartz, kaolinite and boehmite mineral. The boehmite may have been formed from the leachate of detrital sediment, including volcanic ash, rich in Al and precipitated as authigenic boehmite in the underlying coal. REY type in Bangko coal and non-coal samples could be determined to H-type and H-M type. Mostly, REY type of enrichment in Bangko are H-type, owing respectively to the weathered of alkali rich-tonsteins (volcanic ash controlled) and surface water effects.

**Keywords:** Indonesia low rank coal, Muara Enim formation, tonstein, volcanic ash

# The petrographic analysis of waste generated during the gasification process

**Bielowicz, Barbara**

Faculty of Geology, Geophysics and Environmental Protection, AGH University of Science and Technology, Kraków, Poland

The bituminous coal from the Janina deposit has been subjected to the gasification process in an atmospheric CFB (circulating fluidized bed) gasification reactor using CO<sub>2</sub> as a gasifying agent. The gasification process has been performed in the Institute for Chemical Processing of Coal in Zabrze. The gasification was carried out at 889-980°C. Then, the analysis of the combustion process of coal and char resulting from the gasification of bituminous coal in the "Janina" coal mine was carried out at the Czestochowa University of Technology. Fluidized bed combustion tests, including oxy-combustion, was performed on chars. The gaseous and solid products of the process were determined. High levels of combustibles, particularly unburned coal, were found in the ashes resulting from the combustion of coal. In the petrographic analysis, coal samples before the gasification, char samples produced during the gasification process, and bottom ash and fly ash samples were used. The collected samples were analyzed using a wavelength dispersive X-ray spectrometer (WDS). The coal samples were examined using a JEOL JXA-8230 superprobe electron microprobe in order to analyze the chemical composition of solids in the micro area (< 1 µm). The elemental composition analysis in the micro area was performed using an energy dispersive spectrometer (EDS X-ray microprobe analysis) for all elements from boron to uranium. The quantitative analysis of the elemental composition using the secondary wavelength-dispersive X-ray spectroscopy (WDS) was performed using five spectrometers. The structure of waste and char was examined using a FEI Quanta 200 FEG Field Emission Scanning Electron Microscope. The mineral composition was determined with qualitative and quantitative X-ray analysis of the samples carried out using a Philips X'pert APD diffractometer.

According to the coal classification, the coal subjected to gasification process is para bituminous (medium-rank D), high-volatile C bituminous coal, a reflectance of 0.55%, total moisture of 18.8%, ash content (dry basis) of 15.8%, volatile matter of 40.44%, and net calorific value of 19.7 MJ/kg. The petrographic composition is dominated by the vitrinite group (55%). The liptinite group has a share of 9%, the inertinite group: 29%, while mineral matter content is 7%. Pyrite, quartz, kaolinite, siderite, illite, and dolomite are observed in the mineral composition. The char contained 32% of ash (dry basis), 8% of volatile matter (dry, ash free basis), and 0.5% of total moisture. Its net calorific value is 22.2 MJ/kg. The dominant particles in the residues after the gasification process are inertoid and crassinetwork. The macerals from the inertinite group do not change their form during the gasification process. Quartz and dolomite can be observed in the mineral composition. Quartz, illite, hematite, microcline, anhydrite, and amorphous fractions were observed in bottom ash obtained during the combustion of coal. In addition, the presence of magnetite in the fly ash has been confirmed.

Hematite, quartz, anhydrite, and illite were found in the fly and bottom ash resulting from the carbonization process. In the bottom ash, microcline and calcite can be observed, while albite and periclase are present in fly ash. The amorphous fraction is the most frequently observed among all the analyzed samples. The ashes of the "Janina" char are dominated by silicon oxide, amounting up to 30%. The concentration of aluminum oxide (15 - 17%) and iron and calcium oxides is lower. The samples of fly ash were analyzed for the content of combustible matter - coal. The research has confirmed significant amounts (30%) of unburned coal in ash from the "Janina" char.

**Keywords:** coal, gasification, char, fly ash

# **Comparative Study of Methyldiamondoid abundances as maturity estimates with conventional maturity proxies: Examples from West Texas and Northern South America**

**Carvajal-Ortiz<sup>1\*</sup>, Humberto and Thomas Gentzis<sup>1</sup>**

<sup>1</sup>Core Laboratories, 6316 Windfern Road, Houston, TX 77040, USA

\*presenting author

Diamondoids are a class of cage-like hydrocarbons that are structurally similar to small pieces of diamonds. Their formation from polycyclic precursors parallels their dynamic stability. They naturally occur in virtually every oil and condensate, as well as in source-rock extracts. Their ubiquitous nature in oils and extracts of any thermal maturity and their proven stability with increasing thermal maturity makes them useful as thermal maturity proxies past peak oil window and to identify mixtures of low and high maturity fluids. Therefore, diamondoids are used as an alternative and novel thermal maturity proxy, especially in high thermal-maturity settings, where other maturity indicators (e.g., biomarker ratios) are absent or unreliable. Although the use of diamondoids is relatively novel, two relationships using methyldiamondoids are constantly used to establish thermal-maturity relationships between oils, and between oils and extracts (the methyldiamantane index, MDI), and to identify mixtures of fluids with different thermal maturities (3-+4-methyldiamantane concentration vs. Stigmastane concentration).

The present comparative study shows how methyldiamantane proxies from West Texas oils and extracts (such as those sourced from the Woodford Shale), and in oil samples from Northern South America (Colombia, Ecuador) show overall a very good agreement with classic maturity proxies, such as  $T_{max}$  values from Rock-Eval pyrolysis and vitrinite reflectance (V<sub>Ro</sub>) and fluorescence of organic matter. However, caution is advised when using methyldiamondoid-derived proxies in the presence of drilling-additive contaminants (e.g., oil-based mud or OBM) and of oils and extracts that have experienced biodegradation. The latter is probably a highly unrecognized issue when using methyldiamondoids, which can result in erroneous maturities and mixing interpretations. We recommend, based on the results from the present study, the necessity of a holistic, multi-proxy approach, based on the integration of geochemical-screening, organic petrography, and molecular geochemistry techniques as the best possible solution when dealing with such geochemical conundrums.

**Keywords:** Diamondoids; Methyldiamantane; Thermal Maturity; oil-source rock correlation; Geochemistry

# Mineralogy and geochemistry of the Late Permian No. 5 coals from the Nantong coalfield, Chongqing, southwestern China

Chen, Jian<sup>1\*</sup>, Ping Chen<sup>1</sup>, Duoxi Yao<sup>1</sup> and Youbiao Hu<sup>1</sup>

<sup>1</sup> Anhui University of Science and Technology

\*Presenting author

The Nantong coalfield is one important area of coal production in the southwestern Chongqing of China, immediately adjacent to the Songzao coalfield. Due to the input of geochemically different volcanic ashes, the Songzao coals are highly enriched in Nb, Ta, Zr, Hf, REY, Hg, and Se (Zhao *et al.*, 2015), e.g., the enrichment of Nb, Ta, Zr, Hf, and REEs in the No. 11 coal due to the alkaline volcanic ashes (Dai *et al.*, 2007), and the elevated Sc, V, Cr, Co, Ni, Cu, Ga, Y, Zr, Nb, and REEs in the No. 12 coal derived from mafic tuffs (Dai *et al.*, 2010). Moreover, the leaching of the volcanic claystones in the Songzao Tonghua coal led to the deposition of anatase and rhabdophane (Zhao *et al.*, 2013). However, the geochemistry of both trace elements and REY in the Donglin Nos. 4 and 6 coals from the Nantong coalfield eliminate the impact of various volcanic ashes and terrigenous input from the Kangdian Oldland (Chen *et al.*, 2015). The No. 5 coal, one mineable coalbed in this area, is lack in the information on the mineralogy and geochemistry.

A total of nine samples (including one roof sandstone sample and one floor mudstone sample, and seven coal samples) were collected from the workface of the No. 5 coal in the Nantong Coal Mine. The minerals, major element oxides, and trace elements were analyzed by LTA-XRD in combination with Siroquant software, XRF, ICP-MS, ICP-CCT-MS (As and Se), ISE (F), and DMA-80 Hg analyzer (Hg).

The Nantong No. 5 coal indicates a medium ash and high sulfur coal according to Chinese National Standards (16.01-29.00% and >3.00%) (GB/T15224.1-2004, 2004; GB/T15224.2-2004, 2004). The ash yields and total sulfur of samples in the upper part (NT-5-0, NT-5-1, NT-5-2, and NT-5-3) are higher than that of the lower part (NT-5-4, NT-5-5, and NT-5-6). The volatile matter of Nantong No. 5 coal ranges from 14.66 to 18.25%, averaging 16.82%, suggesting a rank of low volatile bituminous coal (ASTM Standard D388-12, 2012).

The minerals are mainly composed of kaolinite, montmorillonite, quartz, calcite, anatase, and pyrite. Compared to the common Chinese coals (Dai *et al.*, 2012), Be, Cr, Se, Zr, Nb, Mo, Ag, Hf, and Hg are slightly enriched, while F and Ta are enriched in the Nantong No. 5 coal, which differentiates the Donglin Nos. 4 and 6 coals (slight enrichment of Se, F, Hg, Nb, and Ta in the No. 4 coal, and F, Be, Ga, Ge, Zr, Nb, and Ta in the No. 6 coal). The upper part of the No. 5 coal is slightly enriched in Be, F, Se, Mo, and Ta, while the lower is slightly enriched in Li, Be, F, Cr, Ag, Cd, In, Sn, Hf, and Th, enriched in Se, Zr, Nb, and Hg, and significantly enriched in Ta. Dai *et al.* (2011) summarized the geochemical characteristics of silicic (low REEs content but with significant fractionation between LREE and HREE), mafic (high concentrations of Sc, V, Cr, Co, and Ni), and alkali (Nb, Ta, Zr, Hf, Ga, and REEs) tonsteins in the Songzao coalfield. The Nantong No. 5 coal might be influenced by alkali volcanic ashes, which exerted different impacts on the upper and lower part of this coalbed. Lithium, Zr, Nb, Ag, Cd, In, Sn, Hf, Ta, Th, U, and REY are enriched in coal NT-5-4 and floor rock NT-5-7, which may be related to the alkaline volcanic ashes as the Songzao No. 11 coal. The concentration of REY in the Nantong No. 5 coal (averaging 258 mg/kg) is higher than that of Donglin Nos. 4 and 6 (98.8 and 116 mg/kg) and Chinese coals (136 mg/kg). Almost all samples present a common pattern, i.e., a significant negative Eu anomaly, obviously differentiating the Emeishan basalt.

## References

- ASTM Standard D388-12, 2012. Standard classification of coals by rank, ASTM International, West Conshohocken, p. PA.
- Chen J., Chen P., Yao D., Liu Z., Wu Y., Liu W., Hu Y., 2015. Mineralogy and geochemistry of Late Permian coals from the Donglin Coal Mine in the Nantong coalfield in Chongqing, southwestern China. *International Journal of Coal Geology* 149, 24-40.
- Dai S., Zhou Y., Ren D., Wang X., Li D., Zhao L., 2007. Geochemistry and mineralogy of the Late Permian coals from the Songzao Coalfield, Chongqing, southwestern China. *Science in China Series D: Earth Sciences* 50, 678-688.
- Dai S., Wang X., Chen W., Li D., Chou C.-L., Zhou Y., Zhu C., Li H., Zhu X., Xing Y., Zhang W., Zou J., 2010. A high-pyrite semianthracite of Late Permian age in the Songzao Coalfield, southwestern China:

Mineralogical and geochemical relations with underlying mafic tuffs. *International Journal of Coal Geology* 83, 430-445.

Dai S., Wang X., Zhou Y., Hower J.C., Li D., Chen W., Zhu X., Zou J., 2011. Chemical and mineralogical compositions of silicic, mafic, and alkali tonsteins in the late Permian coals from the Songzao Coalfield, Chongqing, Southwest China. *Chemical Geology* 282, 29-44.

Dai S., Ren D., Chou C.-L., Finkelman R.B., Seredin V.V., Zhou Y., 2012. Geochemistry of trace elements in Chinese coals: A review of abundances, genetic types, impacts on human health, and industrial utilization. *International Journal of Coal Geology* 94, 3-21.

GB/T15224.1-2004, 2004. Classification for quality of coal - Part 1: ash, Chinese National Standard, Beijing. General Administration of Quality Supervision, Inspection and Quarantine of the People's Republic of China (in Chinese).

GB/T15224.2-2004, 2004. Classification for coal quality - Part 2: Sulfur content, Chinese National Standard, Beijing. General Administration of Quality Supervision, Inspection and Quarantine of the People's Republic of China (in Chinese).

Zhao L., Ward C.R., French D., Graham I.T., 2013. Mineralogical composition of Late Permian coal seams in the Songzao Coalfield, southwestern China. *International Journal of Coal Geology* 116-117, 208-226.

Zhao L., Ward C.R., French D., Graham I.T., 2015. Major and trace element geochemistry of coals and intra-seam claystones from the Songzao coalfield, SW China. *Minerals* 5, 870-893.

**Keywords:** Mineralogy, Geochemistry, Coal, Chongqing, China

# **The Evolution of Petrophysical Properties during Thermal Maturation: Examples from the Montney and Duvernay Formations, Alberta, Canada**

**Clarke, Katherine<sup>1\*</sup> Christopher Clarkson<sup>1</sup>, Hamed Sanei, Per Pedersen<sup>1</sup>, Amin Ghanizadeh<sup>1</sup>, Atena Vahedian<sup>1</sup>, Behrad Rashidi<sup>1</sup> and Chengyao Song<sup>1</sup>**

<sup>1</sup> Department of Geoscience, University of Calgary

<sup>2</sup> Geological Survey of Canada-Calgary, Calgary, Canada

\*presenting author

Rock-Eval pyrolysis is a standard technique used to evaluate the hydrocarbon-generating potential of a formation by quantifying its organic matter content and thermal maturity. By utilizing a new Rock-Eval procedure, in which the heating rate is slowed down over an extended temperature range, previous studies (Sanei *et al.* 2015) have demonstrated that different hydrocarbon components can be more easily distinguished because of enhanced peak resolution. Until now, the effect of this new pyrolysis procedure on petrophysical properties of the rock have not been quantified; a study of this nature may provide insight into the impact of various types of organic matter on reservoir quality.

It is therefore the aim of this project to observe the evolution of organic matter and petrophysical properties of tight formations during pyrolysis using this new Rock-Eval procedure. Specifically, the effects of differing hydrocarbon components on the pore network and reservoir quality are determined, and the evolution of porosity, pore-size distribution, internal surface area, and permeability during this pyrolysis procedure are quantified.